Draft version July 14, 2015
Preprint typeset using LaTeX style emulateapj v. 12/16/11

.

C/O IN PROTOPLANETARY DISKS: THE EFFECT OF RADIAL DRIFT AND VISCOUS ACCRETION

Ana-Maria A. Piso[1], et al

Draft version July 14, 2015

ABSTRACT

...

1. INTRODUCTION

Paragraph 1: introduce the topic, context and its relevance in the big picture. Gas giants are important. The chemical composition of their atmospheres constraints their formation and evolution. Is is therefore important to understand the disk well enough to (1) predict what kind of planet compositions result from planet formation in different parts of the disk, and (2) backtrack the planet formation location based on planet composition.

Main sequence stars commonly host giant planets (refs). The chemical composition of gas giant atmospheres can provide important constraints on their formation, accretion and migration history. *Add the rest as outlined above.*

Paragraph 2: disks are complex, a lot of dynamical and chemical processes going on. However, we have detections of organic molecules. We have detections of snowlines. We see complex chemistry and many molecules we can study.

In recent years, the onset and development of sensitive infrared and (sub)millimeter spectroscopic observations has facilitated the detection of organic molecules in the outer regions of protoplanetary disks (e.g., Öberg et al. 2010, Öberg et al. 2011c, Öberg et al. 2011b, ...). Of particular importance are volatile compounds, since the location of their snowlines determines their relative abundance in gaseous and solid form in the protoplanetary disk, and thus the chemical composition of nascent giant planets. *Add part about snowlines, complex chemistry, many molecules.*

Paragraph 3: let's focus on one (set of) molecules: the C/O ratio. It's an important signature of atmospheric chemistry. While we cannot detect it directly in disks, we have observations in giant planet atmospheres. It's different than stellar. Why? Possible explanation based on snowlines.

Start with the fact that we can't see C/O in disks directly. Then transition to planet atmospheres and modify the next sentence to follow up logically. Notably, an important signature of giant planets atmospheric chemistry is the carbon to oxygen (C/O) ratio. Spectroscopic observations of gas giants such as WASP-12b have found atmospheric C/O ratios close to unity, substantially different from the Solar value of 0.54 (Madhusudhan et al. 2011). One explanation for this discrepancy was proposed by Öberg et al. (2011a), who considered the fact that the main carries of carbon and oxygen, i.e. H_2O, CO_2 and CO, have different condensation temperatures. This changes the relative abundance of C and O in gaseous and solid form as a function of the snowline location of the volatiles mentioned above. Öberg et al. (2011a) calculated analytically the C/O ratio in gas in dust as a function of semimajor axis for passive protoplanetary disks and reproduced a gas C/O ratio of order unity between the CO_2 and CO snowlines, where oxygen gas is highly depleted.

Paragraph 4: the static disk model is a great start, but there are additional dynamical and chemical processes to take into account. Several studies have done that in some form or another — cite Ali-Dib+14, Madhusudhan+14, Thiabaud+15. Briefly discuss their assumptions.

Paragraph 5: finally introduce our goal for this paper: study the dynamical effects such as drift and gas accretion. State our goals: understand the detailed qualitative and quantitative effect of drift and gas accretion on snowline locations, obtain a limit on how far in can the snowlines be pushed, and see how that affects the C/O ratio throughout the disk. State that our specific goals motivate the use of a simplified model (in other words, why what we are doing is different from the studies cited in the previous paragraph).

This needs some restructuring and additions along the lines discussed above. In order to obtain more realistic estimates for C/O ratios across protoplanetary disks, dynamical processes and the disk evolving chemistry have to be taken into account. In this paper, we enhance the model of Öberg et al. (2011a) considering two additional dynamic effects: (1) the radial drift of solids throughout the protoplanetary disk, and (2) the viscous accretion of the disk gas onto the host star. Our goal is two-fold: (1) to quantify the effect of radial drift of solids of different sizes on the location and shape of H_2O, CO_2 and CO snowlines, and (2) to calculate the resulting C/O ratio in gaseous and solid form throughout an actively accreting protoplanetary disk as a function of the grain size distribution and the evolutionary time of the nebula.

This paper is organized as follows: *(section summaries)*.

2. MODEL ASSUMPTIONS

We present our protoplanetary disk model for both a passive and an active disk in section 2.1. In section 2.2, we describe our analytic model for the radial drift of solids. We summarize our ice desorption model in section 2.3. Finally, we discuss the relevant timescales for

[1] Harvard-Smithsonian Center for Astrophysics, 60 Garden Street, Cambridge, MA 02138

dynamical effects in the desorption process in section 2.4.

2.1. *Disk Model*

Passive disk. We adopt a minimum mass solar nebula (MMSN) disk model for a passive disk similar to the prescription of Chiang & Youdin (2010). The gas surface density and midplane temperature are

$$\Sigma_{\rm d} = 2200\,(r/{\rm AU})^{-1}\ {\rm g\ cm^{-2}} \quad (1a)$$

$$T_{\rm d} = 120\,(r/{\rm AU})^{-3/7}\ {\rm K}, \quad (1b)$$

where r is the semimajor axis. Based on some observations of protoplanetary disks (Andrews et al. 2010), our surface density profile, $\Sigma_{\rm d} \propto r^{-1}$, is flatter than that of Chiang & Youdin (2010), i.e. $\Sigma_{\rm d} \propto r^{-3/2}$.

Actively accreting disk with passive temperature profile. We model the active disk as a thin disk with an α-viscosity prescription (Shakura & Sunyaev 1973):

$$\nu = \alpha c_{\rm d} H_{\rm d}. \quad (2)$$

Here ν is the kinematic viscosity, $\alpha < 1$ is a dimensionless coefficient and we choose $\alpha = 0.01$, and $c_{\rm d}$, $H_{\rm d}$ are the isothermal sound speed and disk scale height, respectively:

$$c_{\rm d} = \sqrt{\frac{k_{\rm B} T_{\rm d}}{\mu m_{\rm p}}} \quad (3a)$$

$$H_{\rm d} = \frac{c_{\rm d}}{\Omega_{\rm k}}, \quad (3b)$$

where $k_{\rm B}$ is the Boltzmann constant, μ is the mean molecular weight of the gas, $m_{\rm p}$ is the proton mass, and $\Omega_{\rm k} \equiv \sqrt{GM_*/r^3}$ is the Keplerian angular velocity, with G the gravitational constant and M_* the stellar mass. We choose $M_* = M_\odot$ and $\mu = 2.35$, corresponding to the Solar composition of hydrogen and helium. The temperature profile for an active disk is assumed to be the same as for the passive disk and given by Equation (1b). From Equations (2) and (3), the viscosity can thus be expressed as a power-law in radius, $\nu \propto r^\gamma$, with $\gamma = 15/14 \approx 1$ for our choice of parameters. Following Armitage (2010), we define $R \equiv r/r_{\rm c}$ and $\nu_{\rm c} \equiv \nu(r_{\rm c})$, where $r_{\rm c}$ is a characteristic disk radius. We choose $r_{\rm c} = 100$ AU. The gas surface density is then given by the self-similar solution

$$\Sigma_{\rm d}(R,T) = \frac{M_{\rm d}}{2\pi r_{\rm c}^2 R^\gamma} T^{(-5/2-\gamma)/(2-\gamma)} \exp\Big[-\frac{R^{-(2-\gamma)}}{T}\Big], \quad (4)$$

where $M_{\rm d}$ is the total disk mass and

$$T \equiv \frac{t}{t_{\rm c}} + 1 \quad (5a)$$

$$t_{\rm c} \equiv \frac{1}{3(2-\gamma)} \frac{r_{\rm c}^2}{\nu_{\rm c}}, \quad (5b)$$

where t is time. We choose $M_{\rm d} = 0.1 M_\odot$ (e.g., Birnstiel et al. 2012), but we note that our results are insensitive to this choice (see Section 5).

Active disk steady-state solution. Calculating the midplane temperature self-consistently for an active disk is non-trivial, so instead we use the steady-state solution for the surface density and temperature for a thin disk (e.g., Armitage 2010):

$$T_{\rm d}^4 = \frac{3GM_*\dot{M}}{8\pi\sigma r^3} \quad (6a)$$

$$\dot{M} = 3\pi\nu\Sigma_{\rm d}, \quad (6b)$$

where $\dot{M}$, the mass flux, is constant in steady-state [2]. Based on disk observations (e.g., Andrews et al. 2010), we choose $\dot{M} = 10^{-8} M_\odot\ {\rm yr}^{-1}$. We can then easily determine the radial temperature profile from Equation (6a), $c_{\rm d}$ and $H_{\rm d}$ from Equation (3), as well as the viscosity ν from Equation (2) for a given α. For consistency, we choose $\alpha = 0.01$ as in the previous case. Finally, we determine $\Sigma_{\rm d}$ from Equation (6b).

Static disk. To compare our results with those of Öberg et al. (2011a), we also use a static disk model, with $\Sigma_{\rm d}$ and $T_{\rm d}$ described by Equations (1a) and (1b). The static model does not take into account gas accretion on to the central star or radial drift of solids (see Section 2.2).

2.2. *Radial Drift*

Solid particles in a disk orbit their host star at the Keplerian velocity $v_{\rm k} \equiv \Omega_{\rm k} r$. The gas, however, experiences an additional pressure gradient, which causes it to rotate at sub-Keplerian velocity (Weidenschilling 1977). Dust grains thus experience a headwind, which removes angular momentum, causing the solids to spiral inwards and fall onto the host star. Small particles are well-coupled to the gas, while large planetesimals are decoupled from the gas. From Chiang & Youdin (2010), the extent of coupling is quantified by the dimensionless stopping time, $\tau_{\rm s} \equiv \Omega_{\rm k} t_{\rm s}$, where $t_{\rm s}$ is

$$t_{\rm s} = \begin{cases} \rho_{\rm s} s/(\rho_{\rm d} c_{\rm d}), & s < 9\lambda/4 \quad \text{Epstein drag} \\ 4\rho_{\rm s} s^2/(9\rho_{\rm d} c_{\rm d} \lambda), & s < 9\lambda/4,\ {\rm Re} \lesssim 1 \quad \text{Stokes drag.} \end{cases} \quad (7)$$

Here $\rho_{\rm d}$ is the gas midplane density, $\rho_{\rm s} = 2\ {\rm g\ cm^{-3}}$ is the density of a solid particle, s is the particle size, λ is the mean free path, and Re is the Reynolds number.

For a passive disk, the radial drift velocity can be approximated analytically as

$$\dot{r} \approx -2\eta\Omega_{\rm k} r \Big(\frac{\tau_{\rm s}}{1+\tau_{\rm s}^2}\Big), \quad (8)$$

where

$$\eta \equiv -\frac{\partial P_{\rm d}/\partial \ln r}{2\rho_{\rm d} v_{\rm k}^2} \approx \frac{c_{\rm d}^2}{2v_k^2} \quad (9)$$

and $P_{\rm d} = \rho_{\rm d} c_{\rm d}^2$ is the disk midplane pressure.

For an active disk, the radial drift velocity has an additional term due to the radial movement of the gas, i.e.

$$\dot{r} \approx -2\eta\Omega_{\rm k} r \Big(\frac{\tau_{\rm s}}{1+\tau_{\rm s}^2}\Big) + \frac{\dot{r}_{\rm gas}}{1+\tau_{\rm s}^2}, \quad (10)$$

where $\dot{r}_{\rm gas}$ is the radial gas accretion velocity and can be expressed as (e.g., Frank et al. 2002)

$$\dot{r}_{\rm gas} = -\frac{3}{\Sigma_{\rm d}\sqrt{r}} \frac{\partial}{\partial r}(\nu\Sigma_{\rm d}\sqrt{r}) \quad (11)$$

[2] Equations (6a) and (6b) are valid when $r \gg R_*$, the stellar radius, which is the regime in which we conduct our study.

with $\Sigma_{\rm d}$ from Equation (4). For the active disk steady-state solution (see Section 2.1), $\dot{r}_{\rm gas}$ can be expressed more simply using the definition of the mass flux, $\dot{M} = -2\pi r \dot{r}_{\rm gas}\Sigma_{\rm d}$, with $\dot{M}$ fixed and $\Sigma_{\rm d}$ obtained from Equation (6b).

2.3. *Volatile Desorption*

In order for a volatile species to thermally desorb, it has to overcome the binding energy that keeps it on the grain surface. Following Hollenbach et al. (2009), the desorption rate per molecule for a species x can be expressed as

$$R_{\rm des,x} = \nu_x \exp\left(-E_x/T_{\rm grain}\right), \tag{12}$$

where E_x is the adsorption binding energy, $T_{\rm grain}$ is the grain temperature, and $\nu_x = 1.6 \times 10^{11}\sqrt{(E_x/\mu_x)}$ is the molecule's vibrational frequency, with μ_x the mean molecular weight. We assume that the dust and gas have the same temperature in the disk midplane, hence $T_{\rm grain} = T_{\rm d}$. For H_2O, CO_2 and CO, the binding energies E_x are assumed to be 5800 K, 2000 K and 850 K, respectively (Öberg et al. 2011a). We use the desorption rate, $R_{\rm des}$, to estimate the desorption timescale for particles of different sizes as described in section 2.4.

2.4. *Relevant Timescales*

We can estimate the extent to which radial drift and gas accretion affect desorption by comparing the timescales for desorption, drift and accretion, for solids of different sizes and compositions.

Desorption timescale. We assume that the solid bodies are perfect spheres and are entirely composed of only one volatile species, i.e. either H_2O, CO_2 or CO [3]. The desorption timescale can then be estimated as

$$t_{\rm des} = \frac{\rho_{\rm s}}{3\mu_x m_{\rm p}} \frac{s}{N_x R_{\rm des,x}}, \tag{13}$$

where $N_x \approx 10^{15}$ sites cm^{-2} is the number of adsorption sites of volatile x per cm^2 (Hollenbach et al. 2009).

Radial drift timescale. To order of magnitude, the radial drift timescale can be estimated as

$$t_{\rm r,drift} \sim \frac{r}{\dot{r}}, \tag{14}$$

where $\dot{r}$ is the radial drift velocity given by Equation (8) for a passive disk and by Equation (10) for an active disk.

Gas accretion timescale. The timescale for gas accretion onto the central star for an active disk is (e.g., Armitage 2010)

$$t_{\rm gas,acc} \sim \frac{r^2}{\nu} \sim \frac{1}{2\alpha\eta\Omega_{\rm k}}, \tag{15}$$

with the latter expression derived from Equations (2) and (9).

For simplicity purposes, we calculate the radial drift timescale, $t_{\rm r,drift}$, for a passive disk in this section, but most of our conclusions hold true for an active disk as well. Figure 1 shows $t_{\rm des}$, $t_{\rm r,drift}$ and $t_{\rm gas,acc}$ as a function of particle size at three different locations in the disk, corresponding to the H_2O, CO_2 and CO snowlines in the static disk. As expected, micron-sized particles desorb on very short timescales of $\sim 1-1000$ years in the close vicinity of their respective snowlines, since the desorption rate depends exponentially on temperature and hence on disk location (see Equation 12). On the other hand, their radial drift timescale exceeds the typical disk lifetime of a few Myr by several orders of magnitude due to their strong coupling with the gas. Thus for small particles in a passive disk, the snowline locations and the C/O ratio are the same as for a static disk (see Figure 1 from Öberg et al. 2011a) [4]. At the other extreme, kilometer-sized particles are unaffected by gas drag and have long desorption timescales ($\gg$1 Myr), and the snowline locations and C/O ratio remain unchanged in this case as well. This is true for both passive and active disks, since large planetesimals are decoupled from the gas and hence unaffected by gas accretion onto the host star.

Of particular interest for our purposes is the particle size regime for which $t_{\rm r,drift} \lesssim t_{\rm des} \lesssim t_{\rm d}$ or $t_{\rm gas,acc} \lesssim t_{\rm des} \lesssim t_{\rm d}$, where $t_{\rm d} = 3$ Myr is the disk lifetime. In these cases, radial drift or gas accretion (or both) are faster than thermal desorption. Particles of sizes that satisfy these requirements will drift significantly due to radial drift or gas accretion before desorbing, thus moving the H_2O, CO_2 and CO snowlines closer towards the central star and changing the C/O ratio throughout the disk. We quantify these effects in sections 3 and 4.

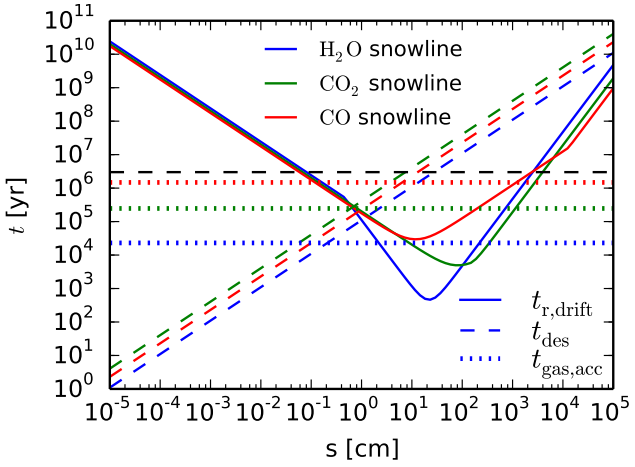

FIG. 1.— Relevant timescales for dynamical effects in the desorption process: $t_{\rm r,drift}$ (solid lines), $t_{\rm des}$ (dashed lines) and $t_{\rm gas,acc}$ (dotted lines). The timescales are calculated at three representative locations, i.e. the H_2O, CO_2 and CO snowlines in the static disk. For our choice of parameters, the snowlines are located at ~0.7 AU (blue lines), ~8.6 AU (green lines) and ~59 AU (red lines), respectively. The horizontal dashed line represents a typical disk lifetime of 3 Myr. Radial drift and gas accretion affect desorption in the regions where their respective timescales, i.e. $t_{\rm r,drift}$ and $t_{\rm gas,acc}$, are comparable to the desorption timescale $t_{\rm des}$.

3. SNOWLINE LOCATIONS

In this section we use the model described in section 2 to quantify the effects of radial drift (passive disk) or ra-

[3] We discuss the validity of these simplifications in section 5.

[4] This is not true for an active disk, however, where gas accretion causes even micron-sized particles to drift significantly before desorbing, as we show in section 3.

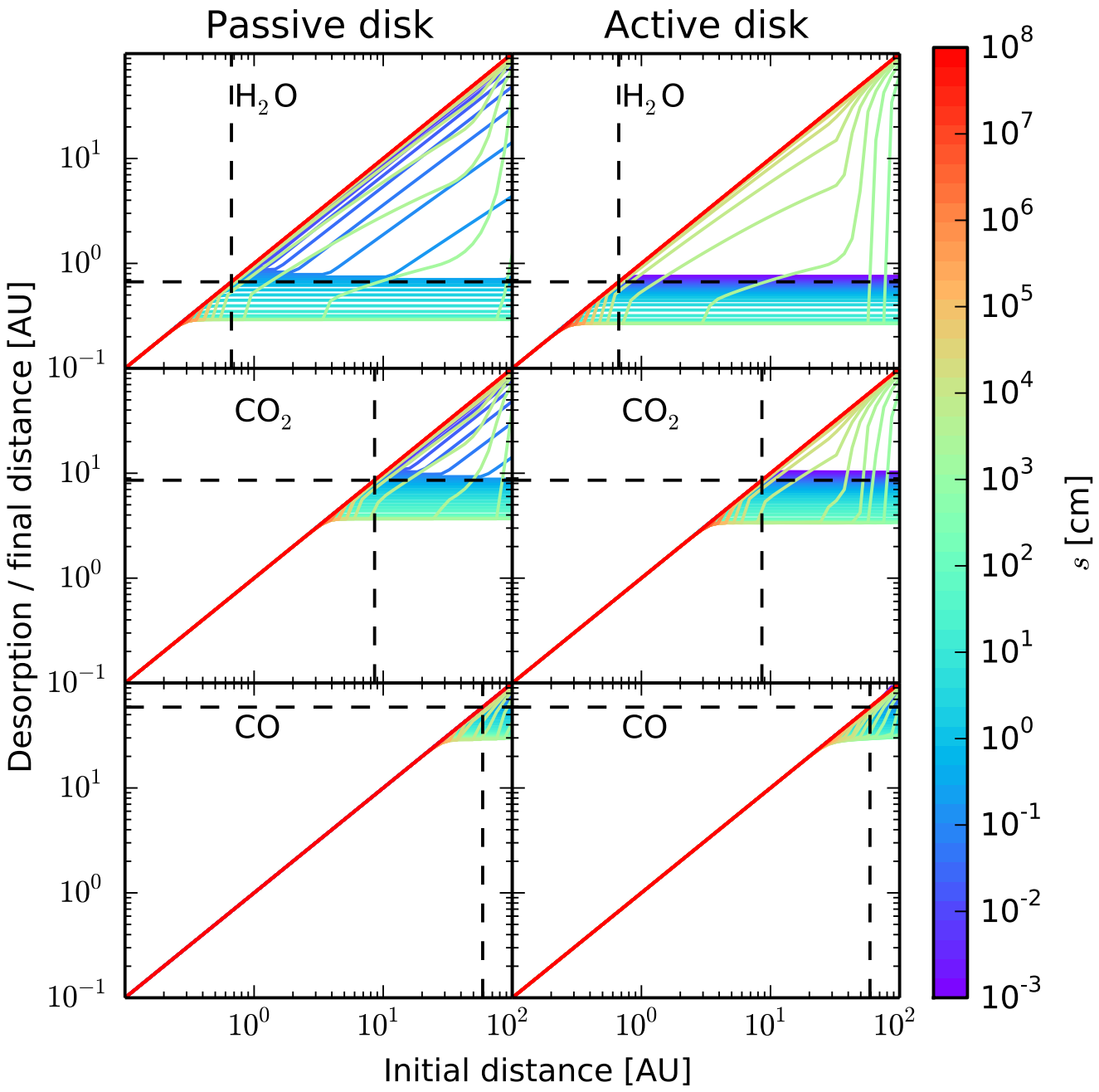

FIG. 2.— Desorption distance as a function of a particle's initial location in the disk, for a range of particle sizes, and for both a passive disk (left panels) and an active disk (right panels). The desorption distance is calculated for particles composed of H_2O (top panels), CO_2 (middle panels) and CO (bottom panels). The particle size increases from 10^{-3} cm to 10^{8} cm as indicated by the color bar. For the range of particle sizes that fully desorb during $t_d = 3$ Myr, the desorption distance is the same regardless of the particles' initial location.

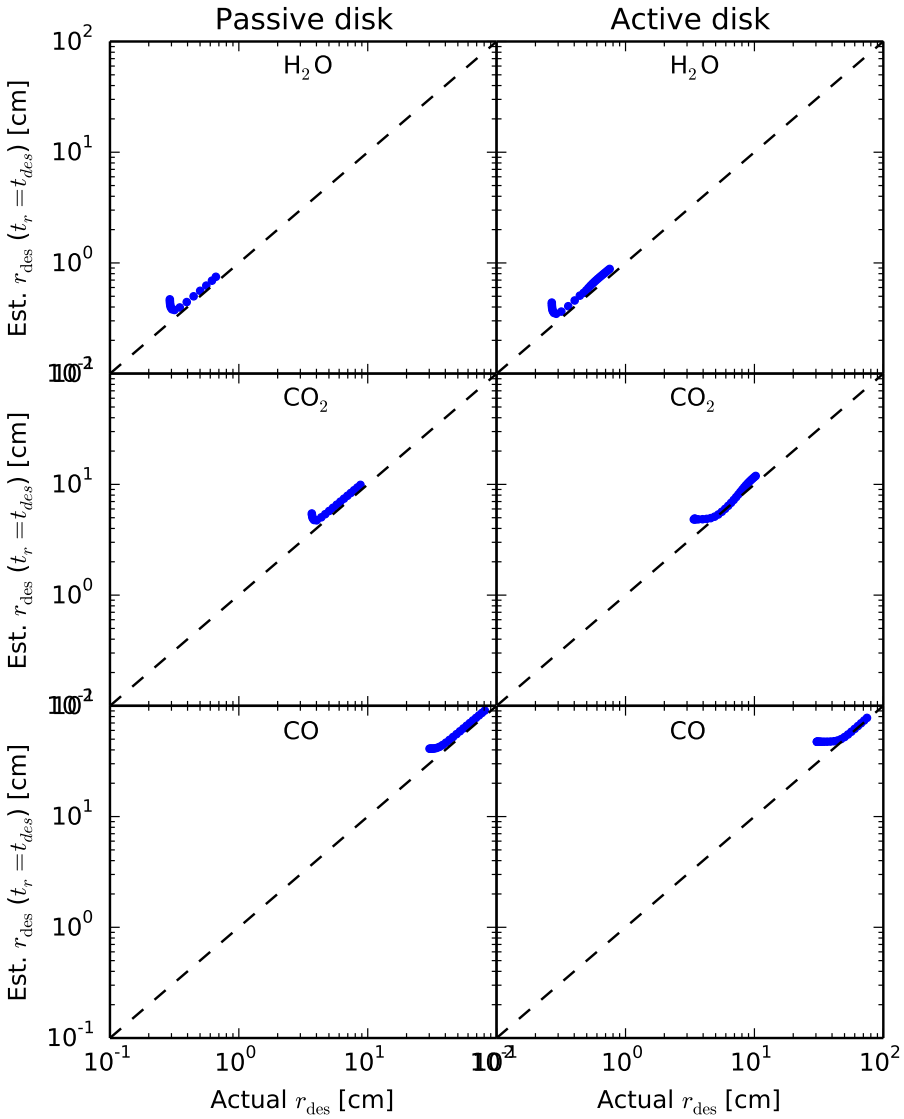

FIG. 3.— Desorption distance estimated from analytic calculations (see text) as a function of the desorption distance calculated numerically, for the range of particle sizes that desorb at a fixed distance regardless of their initial location (see Figure 2 and text). The estimate is performed for a passive disk (left panels) and an active disk (right panels). The particles are composed of H_2O (top panels), CO_2 (middle panels) and CO (bottom panels). The analytic approximation is in good agreement with the numerical result for most cases.

dial drift and gas accretion (active disk) on the snowline location, for dust particles of different sizes composed of either H_2O, CO_2 or CO. Specifically, we determine a particle's final location (i.e., where the particle either fully desorbs or remains at its initial size due to a long desorption timescale) as a function of its initial position in the disk, after the gas disk has dissipated. The disk lifetime, $t_{\rm d}$, is particularly relevant since this is the timescale on which giant planets form. The snowline locations at $t = t_{\rm d}$ throughout the protoplanetary disk determine the disk C/O ratio in gas at this time, and thus the C/O ratio in giant planet atmospheres that have formed *in situ*.

For each species x, we determine the final location in the disk of a particle of initial size s_0 by solving the following system of coupled differential equations:

$$\frac{ds}{dt} = -\frac{3\mu_x m_{\rm p}}{\rho_{\rm s}} N_x R_{\rm des,x} \quad (16a)$$

$$\frac{dr}{dt} = \dot{r}, \quad (16b)$$

where the desorption rate $R_{\rm des,x}$ for each particle type (i.e., composed of H_2O, CO_2 or CO) is evaluated at $T = T_{\rm d}(r)$, and the radial drift velocity $\dot{r}$ is given by Equation (8) for a passive disk and Equation (10) for an active disk. Equations (16a) and (16b) describe the coupled desorption and radial drift, and can be derived straightforwardly from Equation (13). Our boundary conditions are $s(t_0) = s_0$, $r(t_0) = r_0$, and $s(t_{\rm d}) = 0$, where t_0 is the initial time at which we start the integration and r_0 is the initial location of the particle. We choose $t_0 = 1$ year, but our result is independent on the

initial integration time as long as $t_0 \ll t_d$.

As we show in Section 4, a drifting particle that desorbs will do so almost instantaneously and will lose most of its mass very close to the distance at which it fully evaporates. Thus a particle's final location will depend on whether a grain initially at a certain distance is completely desorbed or not within the disk lifetime of 3 Myr. For example, larger grains take longer to desorb and hence are more likely to not evaporate fully in a given timeframe.

Figure 2 shows our results for H_2O, CO_2 and CO particles, for both a passive and an active disk. We do not show the equivalent result for the steady-state active disk since the trends are qualitatively the same as for the active disk with the temperature profile given by Equation (1b). Kilometer-sized bodies do not drift or desorb during the disk lifetime neither for a passive nor for an active disk. Similarly, micron- to mm-sized particles in the passive disk do not drift or desorb unless they are located inside the static snowlines. This is not in contradiction with the desorption timescales for small particles from Figure 1, since small grains only desorb fast at or nearby their respective snowlines, as mentioned in Section 2.4. In an active disk, however, micron-to mm-sized grains do drift significantly since they move at the same velocity as the accreting gas. For 0.5 cm $\lesssim s_0 \lesssim$ 700 cm in a passive disk and 0.001 cm $\lesssim s_0 \lesssim$ 700 cm in an active disk, we notice that particles of initial size s_0 desorb at a fixed distance r_{des} regardless of their original location in the disk. In fact, the only grains that will both drift and evaporate are those that reach their fixed final location (represented by the horizontal curves in Figure 2) within the disk lifetime. We show in section 4 that this result is essential in determining the C/O ratio throughout the disk for different particle sizes.

Intuitively, this fixed r_{des} should be the location in the disk for which $t_{r,drift} \sim t_{des}$, given an initial particle size. We can calculate this location analytically by equating Equations (13) and (14) and solving for $r = r_{des}(s)$ for a given particle size s. Figure 3 shows r_{des} calculated analytically using the prescription above as a function of the actual desorption distance calculated numerically, for the range of particle sizes that desorb at a fixed distance in a passive and an active disk (see Figure 2). We notice that the analytic approximation accurately reproduces the numerical result for most cases of interest, but it slightly deviates for smaller particles. *I've yet to figure out why there is a discrepancy for the small grains. I'll keep thinking about it, but for now I'll leave it as it is since I don't want to give a false explanation just to have one.*

4. RESULTS FOR THE C/O RATIO

We now use our model and the results of Section 3 to determine the H_2O, CO_2 and CO snowline locations and the C/O ratio in disks with static chemistry that experience radial drift of solids and gas accretion on to the central star. In Section 3, we showed that solid particles that drift and fully desorb during the lifetime of the protoplanetary disk do so (1) instantaneously, and (2) at a fixed stellocentric distance, regardless of their initial location in the disk. Figure 4 confirms both of these effects. The left panels show the size evolution with time for H_2O particles of various initial sizes, starting at three different initial locations in a passive disk [5]. Indeed, the solid H_2O particles evaporate almost instantly, although the time t_{des} at which a particle of a given initial size desorbs depends on its initial distance. A particle located at the initial time t_0 at a distance such that $t_{des} > t_d$ will therefore not desorb during the disk lifetime. However, our model assumes that particles drift continuously at any location in the disk. Therefore, a particle that can fully desorb during the disk lifetime for at least one initial location will always desorb, at a fixed distance as discussed in Section 3 and displayed in Figure 2. The right panels of Figure 4 show that the drifting grains lose most of their mass in a very narrow distance range; moreover, this distance is the same for a given initial particle size, no matter where the particle started drifting at the time t_0 when the simulation is started. Figure 4 thus proves claims (1) and (2) above. It follows that the H_2O, CO_2 and CO snowlines are fixed for a given initial particle size and disk model (passive or active). The C/O ratio will then only depend on disk properties, grain size, and the abundance of H_2O, CO_2 and CO relative to the H_2 abundance in the disk midplane.

We use the relative number densities of C and O in their different molecular forms (H_2O, CO_2 and CO) from Table 1 of Öberg et al. (2011a). *Is it necessary to reproduce that table? Seems a bit redundant.*. Figure 5 shows the C/O ratio in gas and dust as a function of semimajor axis for a passive disk, an active disk with a passive temperature profile, and a steady-state active disk *(not yet there)*. The C/O ratio for a static disk is shown as a guideline. The plot is consistent with Figure 2. For the passive disk, only grains larger than ∼0.5 cm drift, desorb and thus form a snowline. In contrast, even ∼micron-sized grains drift and desorb for the active disk, since they flow towards the host star together with the accreting gas. For the same particle size, the snowline locations are slightly closer to the central star in the active disk, due to the fact that the accreting gas adds an additional component to the drift velocity of the solids (cf. Equation 10). Perhaps the most interesting feature is the fact that the snowlines are pushed inwards as the grain size increases. While the plot only shows the snowlines and C/O ratio for particle sizes up to ∼7 m, we have found that almost kilometer-sized boulders are able to drift and desorb for both the passive and the active disk. However, bodies larger than ∼7 m will evaporate at the same location as the meter-sized planetesimals. Thus the innermost snowlines (depicted in red in Figure 5) set the limit on how close in the H_2O, CO_2 and CO snowlines can be pushed due to radial drift and gas accretion on to the host star. Realistic grain size distributions in disks are dominated by large grains (e.g., D'Alessio et al. 2001, Birnstiel et al. 2012). Therefore, the snowlines produced by the largest drifting solids in our model set the inner limit on the snowline locations and are insensitive to a particular grain size distribution. *There will be 1-2 additional sentences for the third panel, the steady-state disk, once that finishes running.*

5. DISCUSSION AND MODEL LIMITATIONS

[5] Our conclusions remain valid for an active disk and for particles composed of CO_2 or CO.

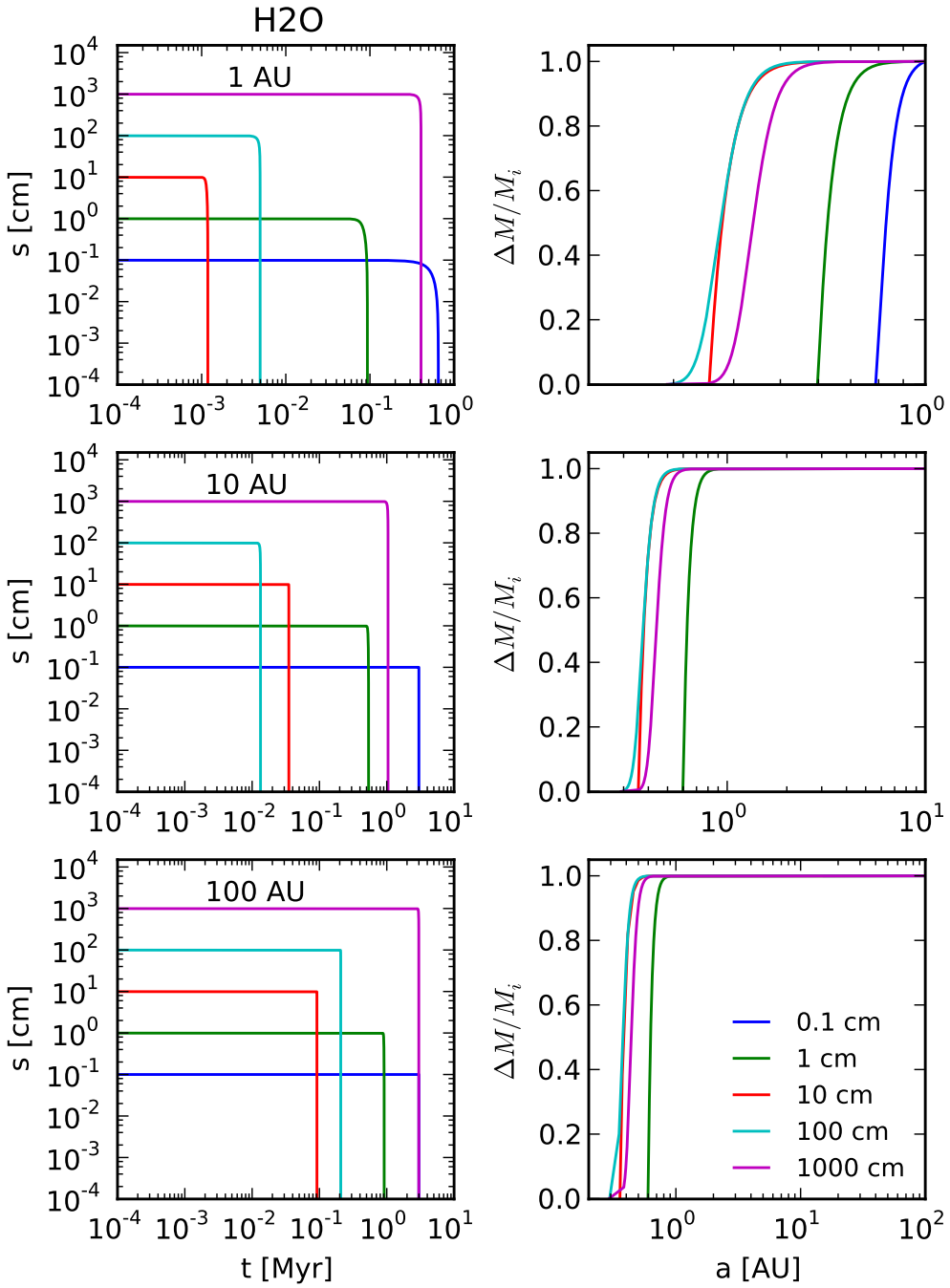

FIG. 4.— Left panels: size of desorbing H_2O particles as a function of time, for different initial particle sizes and for three initial locations in a passive disk: 1 AU (top left), 10 AU (middle left) and 100 AU (bottom left). Particles desorb almost instantaneously. Right panel: fractional mass of the desorbing particles as a function of the particle's location as it drifts, for different initial particle sizes, and at the same initial locations presented in the left panel. Particles lose most of their mass very close to the distance at which they fully desorb.

5.1. *Generality of Results: Dependence on Disk Parameters*

In this section we investigate how variations in our fiducial parameters, such as the total disk mass or the time in the disk evolution at which we determine the snow-

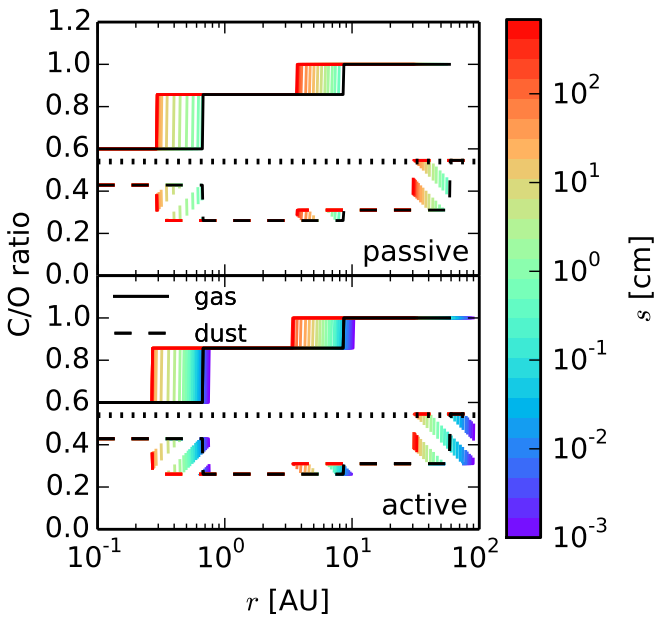

FIG. 5.— C/O ratio in gas (solid lines) and in dust (dashed lines) for a passive disk (top panel) and for an active disk (bottom panel), and for the range of particle sizes that desorb at a fixed distance regardless of their initial location in the disk. The particle size increases from 0.001 cm to ∼700 cm as indicated by the color bar. The horizontal dotted line represents the stellar value of 0.54. The black lines represent the C/O ratio in gas (solid black line) and dust (dashed black line) for a static disk. The snowline location moves inward as the particle size increases. *Some additional text for the currently non-existent third panel.*

line locations and the C/O ratio, affect our results. The disk lifetime $t_{\rm d} = 3$ Myr is the most representative for our calculations, as this is the timeframe in which giant planets accrete their gaseous atmospheres (e.g., Pollack et al. 1996, Piso & Youdin 2014). However, protoplanetary cores start acquiring their envelope at earlier times, before the core is fully formed (e.g., Rafikov 2006). Recent models such as aerodynamic pebble accretion (Lambrechts & Johansen 2012) suggest rapid core growth on timescales of 10^5 years, which implies that the time when cores accrete their massive envelope may be at least an order of magnitude shorter than the disk lifetime. The composition of giant planet atmospheres, and specifically their C/O ratio, can thus depend on the abundance of H_2O, CO_2 and CO in gas and dust forms at earlier times than $t_{\rm d}$ in the disk evolution.

Figure 6 shows the desorption or final distance as a function of a particle's initial location in the disk, for grains of initial sizes of 10 cm and 1 m, composed of either H_2O, CO_2 or CO. These sizes are representative since radial drift timescales are shortest for particles within this size range (see Figure 1) — these are the particles whose drift and desorption evolution should be most strongly affected by variations in disk conditions. We perform the simulations at four representative timescales in the disk evolution to see how the snowline locations evolve with time and affect the C/O ratio. Particles that start at large stellocentric distances do not desorb within the shorter timeframes, e.g. 10^4 or 10^5 years. However, they do evaporate if their initial location is closer to the host star. As stated in Section 4, this implies that the grains form a snowline even after 10^4 years. More importantly, for a given initial grain size, the snowline locations are independent of the time elapsed. Therefore, our results are not only valid at $t_{\rm d}$, but also throughout the earlier time evolution of the protoplanetary disk.

TABLE 1
DYNAMICAL AND CHEMICAL PROCESSES THAT AFFECT THE SNOWLINE LOCATIONS OF THE MAIN C AND O CARRIERS, H_2O, CO_2 AND CO. THE ARROWS SIGNIFY THE DIRECTION IN WHICH A PARTICULAR PROCESS AFFECTS THE SNOWLINES: ← MEANS THAT THE SNOWLINE IS PUSHED CLOSER TO THE HOST STAR, → MEANS THAT THE SNOWLINE IS PUSHED FURTHER FROM THE HOST STAR. THE PRESENCE OF BOTH ARROWS MEANS THAT THE PROCESS MAY HAVE BOTH EFFECTS ON THE SNOWLINE LOCATION.

Process	**Effect**
Radial drift	←
Gas accretion	←
Particle growth	→
Turbulent diffusion	→
Particle fragmentation	→ ←
Morphology	→
Particle composition	→ ←
Non-static chemistry	→ ←

We choose as a fiducial model a total disk mass $M_{\rm d} = 0.1 M_\odot$, but this number is not universally valid. From observations of the dust continuum, Andrews et al. (2013) find that a linear scaling $M_{\rm d} \propto M_*$ is reasonable. Giant planets, however, have been detected around small stars (e.g., Montet et al. 2014), which can have masses as low as $M_* \sim 0.1 M_\odot$. We thus explore the effect of disk mass on the location of snowlines. Figure 7 shows the desorption or final distance as a function on the initial location of a H_2O particle with initial size of 1 m, for two total disk masses: $M_{\rm d} = 0.1 M_\odot$, our fiducial model, and $M_{\rm d} = 0.01 M_\odot$. The simulations are stopped after the same timeframes as those in Figure 6. The location of the H_2O snowline is the same for both disks (the same holds true for the CO_2 and CO snowlines). The C/O ratio is thus insensitive to the choice of $M_{\rm d}$. This result also has implications for transition disks, which have inner cavities significantly depleted of dust (e.g., Espaillat et al. 2012). Since the snowline locations are independent of disk mass, we expect transition disks to exhibit the same drift-desorption behavior as standard disks under the simplified assumptions of our model.

5.2. *Neglected Effects*

Our goals in this paper were (1) to gain a detailed qualitative and quantitative understanding of the effect of radial drift and gas accretion on to the central star on snowline locations and the C/O ratio in disks, and (2) to obtain a limit on how close in the snowlines can be pushed due to drift and gas accretion. We have thus used a simplified model and out of necessity neglected potentially significant dynamical and chemical processes. In what follows, we discuss these limitations and their effects. We note that our future work will address some of these issues.

We summarize in Table 1 the potential physical and chemical processes occurring in disks and their effect on snowline locations. For the sake of completion, Table 1

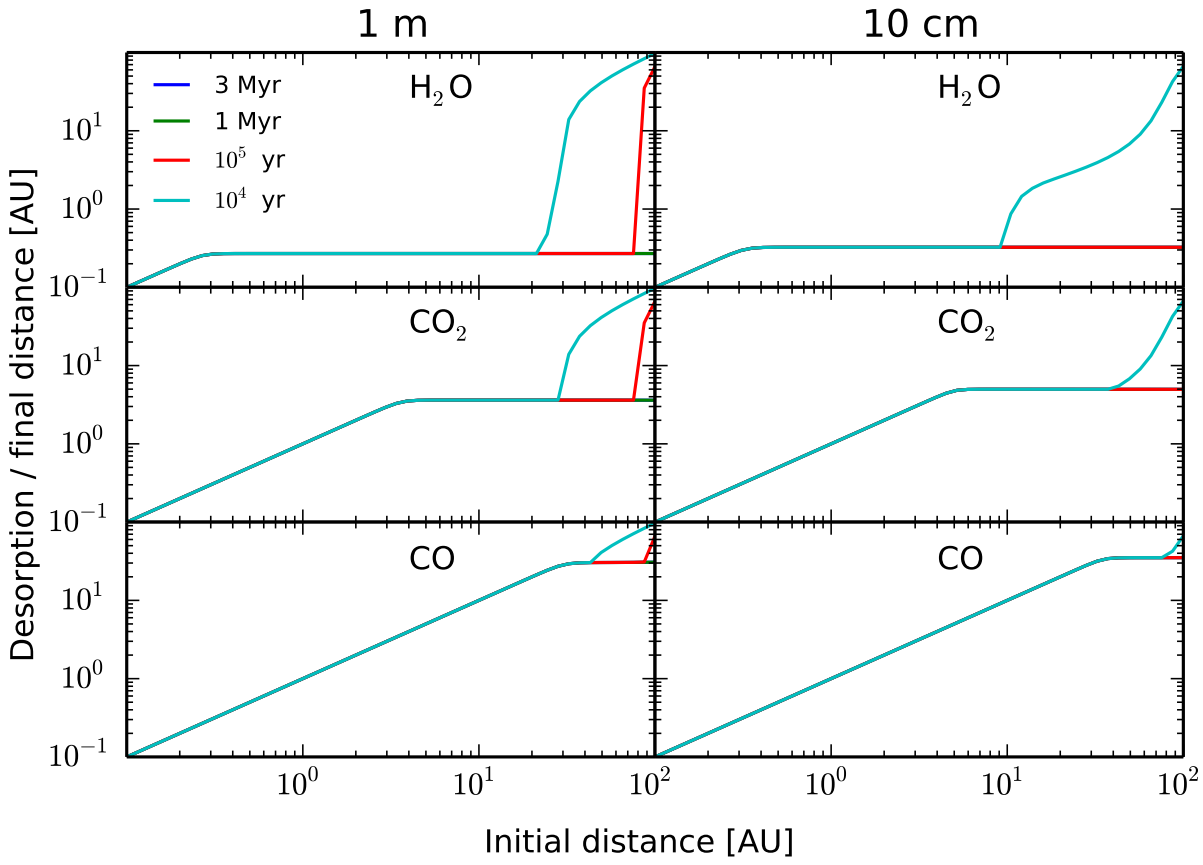

FIG. 6.— Desorption / final distance as a function of initial position in the disk for particles of initial size $s_0 = 1$ m (left panels) and $s_0 = 10$ cm (right panels), for grains composed of H_2O (top panels), CO_2 (middle panels) and CO (bottom panels). The evolution is shown at four representative timescales: 10^4 yr (cyan curve), 10^5 yr (red curve), 1 Myr (green curve), and 3 Myr, the disk lifetime (blue curve). For a given particle size, the desorption distance, and hence the H_2O, CO_2 and CO snowlines, have the same location regardless of the time at which the simulation is stopped.

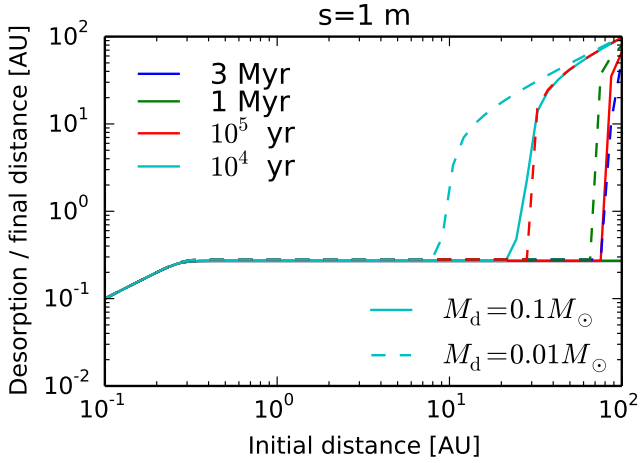

FIG. 7.— Desorption / final distance as a function of initial position in the disk for H_2O particles of initial size of 1 m, for total disk masses $M_d = 0.1 M_\odot$ (solid lines) and $M_d = 0.01 M_\odot$ (dashed lines). The timescales of the simulations and their color code are the same as in Figure 6. A lower disk mass does not change the snowline location.

also includes the processes addressed in this paper, i.e. radial drift and gas accretion. The neglected effects are discussed in more detail below.

1. **Particle growth.** While our model assumes a range of particle sizes, each size is considered fixed for a given grain throughout its drift and evolution. However, grain growth has been observed in protoplanetary disks (e.g., Ricci et al. 2010, Pérez et al. 2012), as well as theoretically constrained (e.g., Birnstiel et al. 2010, Birnstiel et al. 2012). In Section 4 we have shown that larger grains move the snowline locations closer in, but those locations remain fixed above a certain particle size. Once the solids grow larger than km-sized, they are no longer affected by drift or desorption, and the snowline reduces to that of a static disk. It follows that grain growth will eventually push the snowline location outwards.

2. **Turbulent diffusion.** The radial drift model presented in Section 2.2 only considers a laminar flow and thus ignores turbulence. However, the disk gas also experiences turbulent diffusion (e.g., Birnstiel et al. 2012, Ali-Dib et al. 2014). Turbulence causes eddies and vertical mixing, which are likely to reduce the radial gas accretion velocity. Additionally,

the flow of H_2O, CO_2 and CO vapor will diffuse radially, causing it to cross the snowline and refreeze, thus moving the snowline location outwards altogether.

3. **Particle fragmentation.** Frequent particle collisions in disks cause them to fragment (e.g., Birnstiel et al. 2012). The fragmentation of meter- to km-sized particles will move the snowlines outwards, as smaller particles desorb faster and further out from the host star (cf. Figures 2 and 5). Large boulders, which neither drift nor desorb, may become e.g. meter-sized due to collisions and subsequent fragmentation, which will cause them to drift significantly before desorbing, pushing the snowlines inwards. Thus fragmentation can move the snowline locations in either radial direction.

4. **Morphology.** Our model assumes that the ice particles are perfect, homogeneous spheres. However, this is not a very good approximation, since grain growth can be fractal rather than compact (Zsom et al. 2010, Okuzumi et al. 2012). The inhomogeneity due to cracks in the grain structure will cause the particles to desorb faster. They will therefore drift less before evaporating and will move the snowlines outwards.

5. **Particle composition.** The ice particles in our model are assumed to be fully formed of either H_2O, CO_2 or CO. In reality, the grains have a layered structure, such as an interior composed of non-volatile materials (e.g., sillicates) covered by an icy layer. The ice thus only constitutes a fraction of the total particle mass, which accelerates its desorption and pushes the snowlines outwards. The grains may also be composed of a mixture of H_2O, CO_2 and CO ices. The relative fraction of each volatile, as well as their degree of mixing, will determine their desorption timescale, and as a result whether the snowlines are moved towards or away from the central star.

6. **Non-static chemistry.** As the goal of this paper was to explore only the dynamical effects on snowline locations and the C/O ratio in disks, we have assumed a simple, static chemical model. However, gas-grain chemistry is very complex and time-dependent. In the inner disk, chemistry approaches equilibrium due to intense sources of ionizing radiation (e.g., Ilgner et al. 2004), while in the outer disk high energy radiation and cosmic rays are the key drivers of chemistry, which is no longer in equilibrium (e.g., van Dishoeck 2006). A multitude of chemical evolution models have been developed (see references in Henning & Semenov 2013), many of which contain tens or hundreds of chemical reactions. Due to the complexity of these chemical models, most of them are decoupled from disk dynamics. The effect of disk chemistry on snowline locations, shape, time evolution, or the C/O ratio is therefore difficult to estimate. In a future paper, we plan to parametrize the chemical model developed by Merchantz et al. (in preparation) that traces the evolution of the main C and O oxygen carriers, and incorporate it in our radial drift calculation.

6. SUMMARY

To be done soon.

REFERENCES

Ali-Dib, M., Mousis, O., Petit, J.-M., & Lunine, J. I. 2014, ApJ, 785, 125

Andrews, S. M., Rosenfeld, K. A., Kraus, A. L., & Wilner, D. J. 2013, ApJ, 771, 129

Andrews, S. M., Wilner, D. J., Hughes, A. M., Qi, C., & Dullemond, C. P. 2010, ApJ, 723, 1241

Armitage, P. J. 2010, Astrophysics of Planet Formation

Birnstiel, T., Dullemond, C. P., & Brauer, F. 2010, A&A, 513, A79

Birnstiel, T., Klahr, H., & Ercolano, B. 2012, A&A, 539, A148

Chiang, E. & Youdin, A. N. 2010, Annual Review of Earth and Planetary Sciences, 38, 493

D'Alessio, P., Calvet, N., & Hartmann, L. 2001, ApJ, 553, 321

Espaillat, C., Ingleby, L., Hernández, J., Furlan, E., D'Alessio, P., Calvet, N., Andrews, S., Muzerolle, J., Qi, C., & Wilner, D. 2012, ApJ, 747, 103

Frank, J., King, A., & Raine, D. J. 2002, Accretion Power in Astrophysics: Third Edition

Henning, T. & Semenov, D. 2013, Chemical Reviews, 113, 9016

Hollenbach, D., Kaufman, M. J., Bergin, E. A., & Melnick, G. J. 2009, ApJ, 690, 1497

Ilgner, M., Henning, T., Markwick, A. J., & Millar, T. J. 2004, A&A, 415, 643

Lambrechts, M. & Johansen, A. 2012, A&A, 544, A32

Madhusudhan, N., Harrington, J., Stevenson, K. B., Nymeyer, S., Campo, C. J., Wheatley, P. J., Deming, D., Blecic, J., Hardy, R. A., Lust, N. B., Anderson, D. R., Collier-Cameron, A., Britt, C. B. T., Bowman, W. C., Hebb, L., Hellier, C., Maxted, P. F. L., Pollacco, D., & West, R. G. 2011, Nature, 469, 64

Montet, B. T., Crepp, J. R., Johnson, J. A., Howard, A. W., & Marcy, G. W. 2014, ApJ, 781, 28

Öberg, K. I., Murray-Clay, R., & Bergin, E. A. 2011a, ApJ, 743, L16

Öberg, K. I., Qi, C., Fogel, J. K. J., Bergin, E. A., Andrews, S. M., Espaillat, C., van Kempen, T. A., Wilner, D. J., & Pascucci, I. 2010, ApJ, 720, 480

Öberg, K. I., Qi, C., Fogel, J. K. J., Bergin, E. A., Andrews, S. M., Espaillat, C., Wilner, D. J., Pascucci, I., & Kastner, J. H. 2011b, ApJ, 734, 98

Öberg, K. I., Qi, C., Wilner, D. J., & Andrews, S. M. 2011c, ApJ, 743, 152

Okuzumi, S., Tanaka, H., Kobayashi, H., & Wada, K. 2012, ApJ, 752, 106

Pérez, L. M., Carpenter, J. M., Chandler, C. J., Isella, A., Andrews, S. M., Ricci, L., Calvet, N., Corder, S. A., Deller, A. T., Dullemond, C. P., Greaves, J. S., Harris, R. J., Henning, T., Kwon, W., Lazio, J., Linz, H., Mundy, L. G., Sargent, A. I., Storm, S., Testi, L., & Wilner, D. J. 2012, ApJ, 760, L17

Piso, A.-M. A. & Youdin, A. N. 2014, ApJ, 786, 21

Pollack, J. B., Hubickyj, O., Bodenheimer, P., Lissauer, J. J., Podolak, M., & Greenzweig, Y. 1996, Icarus, 124, 62

Rafikov, R. R. 2006, ApJ, 648, 666

Ricci, L., Testi, L., Natta, A., & Brooks, K. J. 2010, A&A, 521, A66

Shakura, N. I. & Sunyaev, R. A. 1973, A&A, 24, 337

van Dishoeck, E. F. 2006, Proceedings of the National Academy of Science, 103, 12249

Weidenschilling, S. J. 1977, MNRAS, 180, 57

Zsom, A., Ormel, C. W., Güttler, C., Blum, J., & Dullemond, C. P. 2010, A&A, 513, A57